Journal of Research in Pharmacy

Research Article

www.jrespharm.com

Development and evaluation of α-arbutin loaded nanostructured lipid carriers for enhanced in-vitro cytotoxic activity in melanoma

Mahmut Ozan TOKSOY [1] *, **İlhan SABANCILAR** [2]

[1] Department of Pharmaceutical Technology, Faculty of Pharmacy, Dicle University, Diyarbakır, Türkiye.
[2] Department of Medical Services and Techniques, Faculty of Health Services, Bitlis Eren University, Bitlis, Türkiye.
* Corresponding Author. E-mail: mozan.toksoy@dicle.edu.tr (MO.T.); Tel. +90-412-241 10 00.

Received: 14 October 2024 / Revised: 14 December 2024 / Accepted: 21 December 2024

ABSTRACT: The aim of this study was to develop and optimize α-arbutin-loaded nanostructured lipid carriers (Ar-NLCs) using the QbD. Additionally, the formulation studies, *in-vitro* and *ex-vivo* performance of Ar-NLCs were assessed, along with their cytotoxic efficacy in melanoma cells. The Ar-NLCs were fabricated using the high-speed homogenization-ultrasonication method, incorporating Gelucire 48/16, Castor oil, Capryol 90, and Tween 80. To analyze the impact of factors on Ar-NLCs, the Box-Behnken design (BBD) was utilized. The Ar-NLCs were characterized by particle size, polydispersity index, morphology, zeta potential, release kinetics, permeation, flux and stability. Additionally, Ar-NLCs cytotoxicity was assessed using the A375 cells. The Ar-NLCs demonstrated a particle size of 228.7 ± 44.5 nm, a zeta potential of -14.2 ± 2.64 mV respectively. The entrapment efficiency was 67.62 ± 4.46%. The α-arbutin release from NLCs followed Weibull kinetics. Notably, Ar-NLCs demonstrated a 2.53-fold higher permeability compared to Ar-SOL. Furthermore, Ar-NLCs exhibited significantly stronger cytotoxic effects against melanoma cells than Ar-SOL. This study reports the successful development of Ar-NLCs using a QbD approach. Enhanced transdermal permeability, enhanced cytotoxicity on melanoma cells, and sustained release of α-arbutin from NLCs were achieved. These findings indicate that NLCs offer a viable alternative drug delivery system for transdermal applications.

KEYWORDS Box-Behnken design; release kinetics; ex-vivo permeation; cytotoxicity; nanostructured lipid carriers

1. INTRODUCTION

Melanin, a pigment accountable for the coloration of the body, hair, and different tissues, is synthesized within melanosomes. Melanocytes play a crucial role in homeostasis and photoprotection of the skin. Dysregulation of melanin metabolism may lead to pigmentary disorders. Several factors can alter the production of melanin such as genetics, hormonal fluctuations, diet, and environmental factors. Melanoma is an aggressive and potentially fatal formation of cancer that originates in melanocytes [1]. Globally, cutaneous melanoma accounts for approximately 232,100 (1.7%) of all newly diagnosed malignant cancers, leading to around 55,500 deaths annually. The primary symptom of malignant melanoma is often the forming of a new mole or observable changes in a current mole [2]. While melanoma is commonly linked to ultraviolet (UV) light exposure from the sun, other risks include both genetic and environmental factors. Although the survival rate of localized cutaneous melanoma is 99%, it drops significantly to 25% for cases with distant metastases [3].

The α-arbutin (Ar) is a natural polyphenol used as a whitening active ingredient in cosmetics because of its ability to inhibit melanin production by blocking the tyrosinase. Beyond its skin-lightening effects, α-arbutin has demonstrated various therapeutic attributes, like antioxidant, antimicrobial, and anti-inflammatory effects, and holds potential as an anticancer agent [4]. Research indicates that α-arbutin exhibits cytotoxicity against various cancer and tumour cell lines. However, α-arbutin's hydrophilic and hygroscopic nature, with a log P value of -1.49, presents challenges for its penetration via the stratum corneum, limiting its ability to reach melanocytes in more in-depth skin layers [5]. To overcome this issue, nano-sized drug carriers are being developed to pass the stratum corneum barrier, enabling the effective delivery of hydrophilic active compounds like α-arbutin to the inner layers of the skin.

How to cite this article: Toksoy MO, Sabancılar İ. Development and evaluation of α-arbutin loaded nanostructured lipid carriers for enhanced cytotoxic activity in melanoma. J Res Pharm. 2025; 29(4): 1712-1725.

ISSN: 2630-6344

https://doi.org/10.12991/jrespharm.1734671

Numerous studies have highlighted the advantages of nanostructured lipid carriers (NLCs) over other lipid-based drug delivery systems like solid lipid nanoparticles (SLNs), liposomes, nanoemulsions, and microemulsions. As second-generation drug carriers, NLCs possess a solid matrix at body temperature. NLCs are formed by physiologically biodegradable and biocompatible lipids and surfactants, which are accepted by regulatory authorities for various drug delivery applications [6]. NLCs exhibit superior properties compared to other colloidal carriers, such as enhanced drug loading and the ability to prevent drug excretion, providing greater flexibility in modulating drug release. The solid and liquid lipid combination in NLCs results less ordered lipid matrix compared to the fully solid lipids used in SLNs. This structural disorder decreases crystallinity and creates "defects" within the nanoparticles, which enhance the loading capacity of drug and reduce the drug expulsion from the NLCs. These unique characteristics make NLCs versatile for various routes of drug administration [7].

Quality by Design (QbD) is a modern product development approach that emphasizes the correlation between quality attributes and process parameters. QbD reduces time, cost, and material waste in formulation development. Although there are many statistical designs, Box-Behnken experimental design (BBD) is often preferred today because it provides savings by using fewer resources, and the parameters affecting the formulation can be examined individually [8].

The aim of this study was to develop and optimize α-arbutin-loaded nanostructured lipid carriers (Ar-NLCs) for enhanced permeability and cytotoxic activity. The permeability, flux, and release kinetics of α-arbutin in NLCs (Ar-NLC) and solution (Ar-SOL) were determined. Additionally, the anticancer activity of α-arbutin and Ar-NLCs were conducted in A375 melanoma cells.

2. RESULTS

2.1. Selection of lipids and surfactants

The solid lipids were selected according to their affinity, while liquid lipids and surfactants were chosen according to their ability to dissolve α-arbutin in high concentrations. The affinities of α-arbutin to Gelucire 48/16 (72.487 ± 6.258%), Precirol ATO 5 (52.355 ± 6.423%), and Compritol ATO 888 (58.635 ± 5.624%) were measured. Gelucire 48/16 was selected as the solid lipid for its highest α-arbutin affinity. The solubility of α-arbutin in Castor oil (2.308 ± 0.114mg/mL), St. John's wort oil (0.587 ± 0.211 mg/mL), and Jojoba oil (1.46 ± 0.124 mg/mL) was determined (Figure 1). As a liquid lipid with the highest solubility of α-arbutin, Castor oil was selected for further studies.

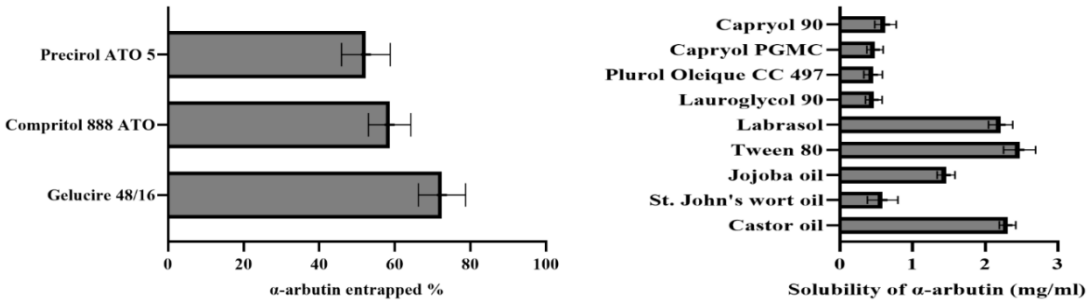

Figure 1. The affinity and solubility of α-arbutin in different lipids, and surfactants.

Further, the solubility values for α-arbutin in Capryol 90, Capryol PGMC, Plurol Oleique CC 497, Lauroglycol 90, Labrasol, and Tween 80 were found as 0.626 ± 0.148 mg/mL, 0.482 ± 0.112 mg/mL, 0.455 ± 0.126 mg/mL, 0.465 ± 0.113 mg/mL, 2.214 ± 0.167 mg/mL, and 2.473 ± 0.223 mg/mL, respectively. As a result, Tween 80 and Capryol 90 were selected as surfactants. The physical examination of the Gelucire 48/16 and castor oil mixture at various ratios (9:1 to 1:9) indicated that a ratio of 8:2 provided optimal miscibility without phase separation.

2.2. Preparation of Ar-NLCs

A 3-factor, 3-response BBD was conducted. The data was presented in Table 1, and equations (Eq. 1-3) given below.

Table 1. Factors and responses according to BBD

Run	Factors			Responses		
	Gelucire 48/16 : Castor oil (8:2, %)	Tween 80 (%)	Capryol 90 (%)	Particle size (nm)	Zeta potential (mV)	PDI
1	20	3	3	214.5	-15.3	0.247
2	30	3	5	268.2	-15.6	0.246
3	10	3	1	163.4	-15.1	0.222
4	30	1	3	279.8	-11.5	0.183
5	20	5	5	194.6	-15.7	0.186
6	20	1	5	207.5	-12.9	0.214
7	20	3	3	226.3	-15.9	0.267
8	20	5	1	143.7	-17.6	0.182
9	30	5	3	293.3	-16.5	0.256
10	10	5	3	176.3	-17.5	0.184
11	20	3	3	230.4	-15.6	0.280
12	10	1	3	159.8	-12.7	0.236
13	20	3	3	215.7	-15.8	0.226
14	30	3	1	284.7	-16.1	0.251
15	20	3	3	223.3	-15.8	0.261
16	20	1	1	193.5	-12.3	0.215
17	10	3	5	168.4	-15.7	0.188

Ps (nm)=$224.04+57.26X_1-4.09X_2+6.68X_3+20.81X_1^2-0.75X_1X_2-5.38X_1X_3-15.54X_2^2+9.23X_2X_3-21.67X_3^2$ (Eq. 1)

PDI= $0.256+0.013X_1-0.005X_2-0.005X_3-0.007X_1^2+0.0313X_1X_2+0.007X_1X_3-0.035X_2^2+0.0013X_2X_3-0.023X_3^2$ (Eq. 2)

Zp (mv)= $-15.68+0.163X_1-2.24X_2+0.15X_3+0.065X_1^2-0.05X_1X_2+0.275X_1X_3+1.07X_2^2+0.625X_2X_3-0.01X_3^2$ (Eq. 3)

According to the ANOVA (Table 2), F-values were 12.24, 3.22, and 18.02 for Ps, PDI, and Zp, respectively. The probability that F-values occurred due to noise was 0.16%, 6.88%, and 0.05% for particle size, PDI, and zeta potential respectively.

Table 2. Coefficients and p-values (ANOVA).

Coefficients	Responses		
	Ps (nm)	PDI	Zp (mV)
Mean	214.32	0.226	-15.15
Standard deviation	17.00	0.0218	0.5392
r^2	0.940	0.805	0.959
Model F-value	12.24	3.22	18.02
Model p-value	0.0016	0.0688	0.0005

The 3D surface-response graphs were created (Figure 2). The effects of Gelucire 48/16:Castor oil, Capryol 90, and Tween 80 amount on the characteristic of NLCs were determined.

The desirability point was acquired. According to this, the NLCs containing Gelucire 48/16:Castor oil (8:2, 16%), Tween 80 (5%), and Capryol 90 (1%) would have the particle size of 143.7 nm, the polydispersity index of 0.182, the zeta potential of -17.56 mV (r^2 = 0.998).

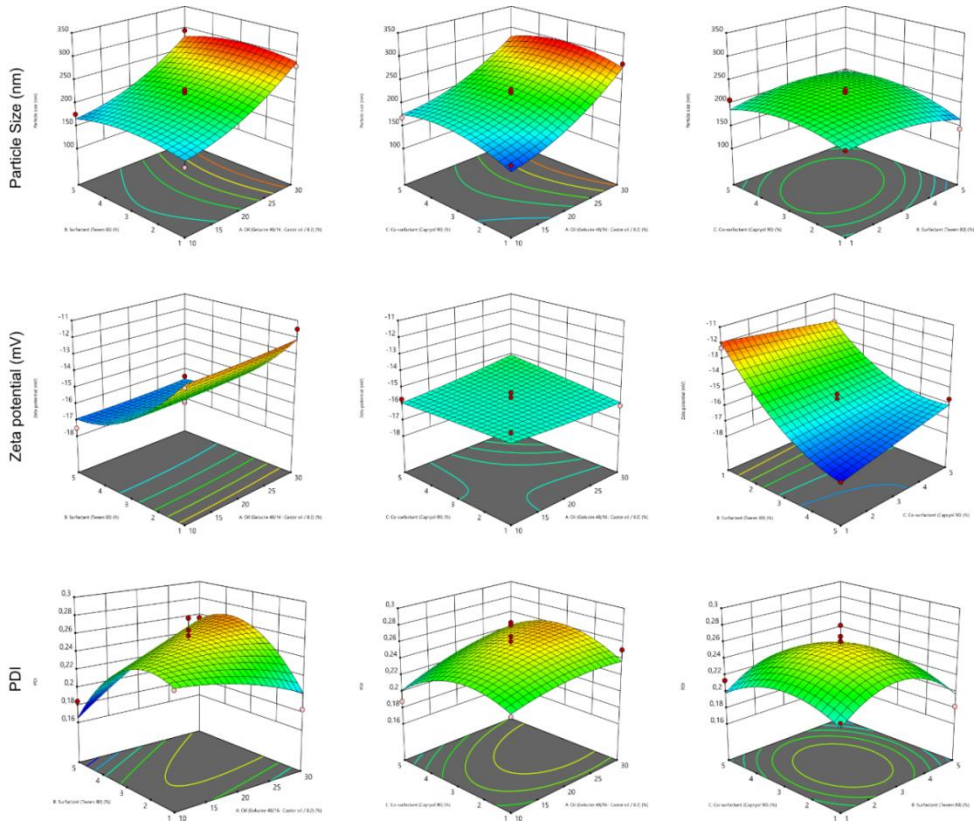

Figure 2. The effects of ingredient ratios on Ar-NLCs

2.3. Characterization studies of the Ar-NLC

After the α-arbutin was loaded on to NLCs, the particle size, PDI, and zeta potential of the optimized Ar-NLCs were determined 228.7 ± 44.5 nm, 0.245 ± 0.03, and -14.2 ± 2.64 mV respectively (Figure 3), (n=3 ± SD). The entrapment efficiency% was 67.62 ± 4.46% (n=3, ± SD).

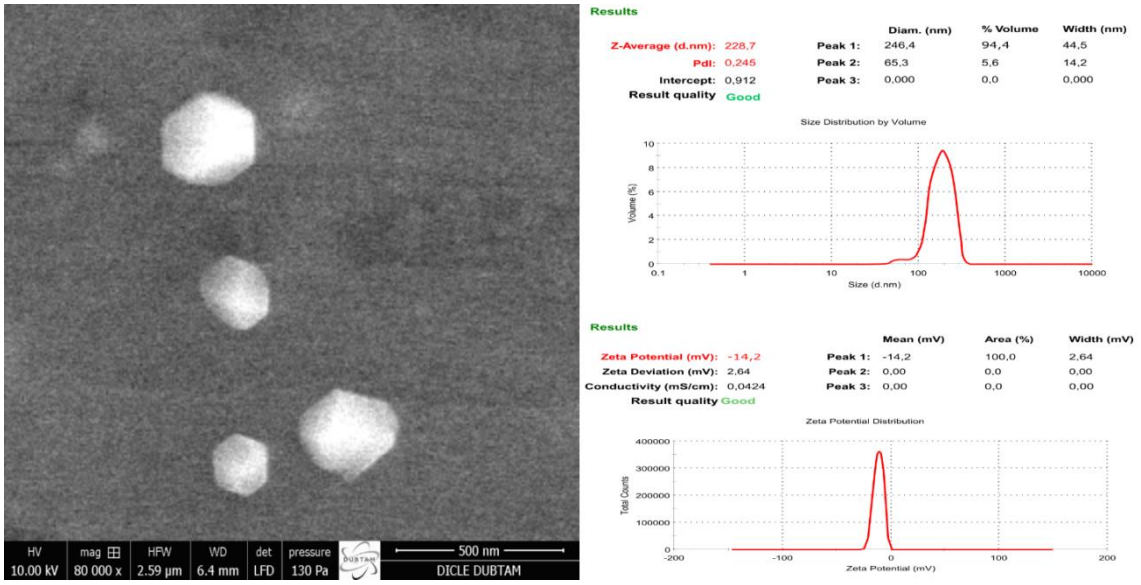

Figure 3. SEM images, particle size, and zeta potential of Ar-NLCs.

The thermograms of the α-arbutin, Gelucire 48/16, and blend of α-arbutin, Gelucire 48/16, and Castor oil were shown in Figure 4. The α-arbutin and Gelucire 48/16 showed an endothermic peak at 204°C and 49°C respectively [9, 10]. DSC thermograms showed no interaction between the compounds.

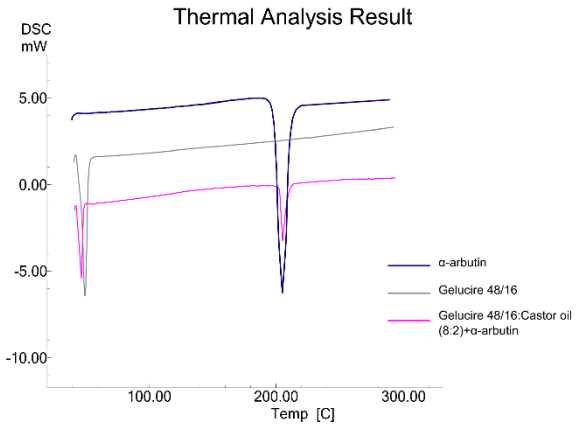

Figure 4. The thermograms (α-arbutin, Gelucire 48/16, and physical blend).

The Fourier transform of α-arbutin (Figure 5d), Gelucire 48/16 (Figure 5a), Castor oil (Figure 5b), Gelucire 48/16:Castor oil (8:2, Figure 5c), and mixture of α-arbutin, Gelucire 48/16 and Castor oil (Figure 5e) was shown. Gelucire 48/16's -OH band (2885 cm^{-1}), C=O band (1736 cm^{-1}) were determined [11]. FTIR spectrum of α-arbutin displayed the O-H stretching (3400-3200 cm^{-1}), aromatic C=C stretching (1513 cm^{-1}) and C-O stretching (1226 cm^{-1}, 1080 cm^{-1} and 1032 cm^{-1}) respectively [9, 10]. Castor oil showed C=O band (1740 cm^{-1}, 2922 cm^{-1}). Also, O-H stretching was observed (3210-3640 cm^{-1}) [12]. In the FTIR studies on the mixture, all major α-arbutin-related peaks were current, suggesting no compound interactions.

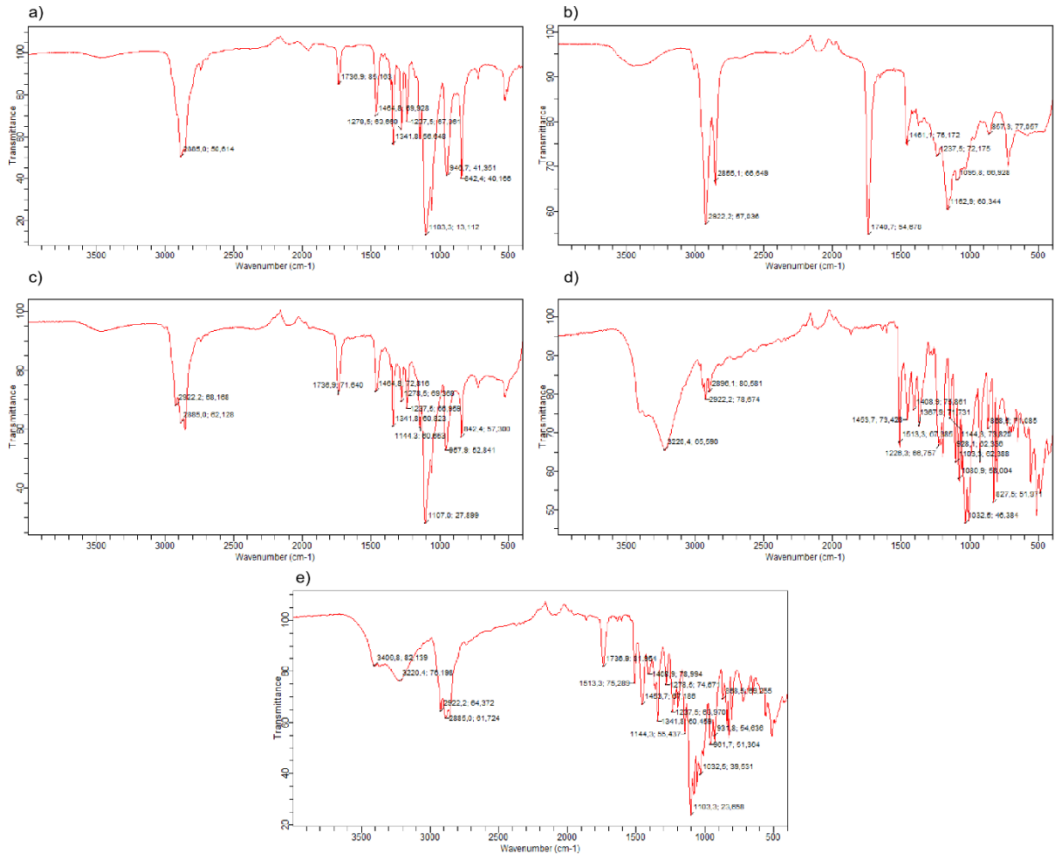

Figure 5. FTIR spectrum of a) Gelucire 48/16, b) Castor oil, c) Gelucire 48/16:Castor oil (8:2), d) α-arbutin, and e) physical blend.

2.4. Investigation of release and kinetics

The cumulative release of α-arbutin from Ar-SOL and Ar-NLCs were evaluated (Figure 6). There was a burst release of α-arbutin in the Ar-NLCs, 26.249 ± 6.139% after 1 hour, pursued by a controlled release with 70.843 ± 9.242% after 12 hours. Additionally, the release kinetics were evaluated (Figure 7 and Table 3).

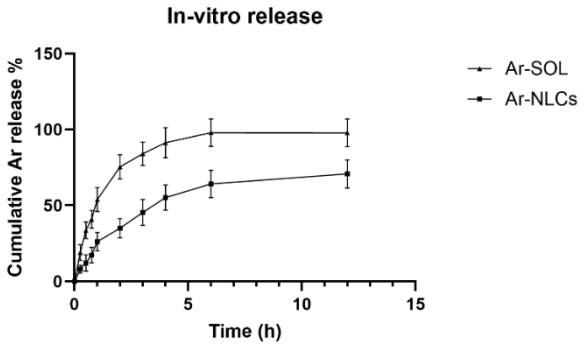

Figure 6. Cumulative α-arbutin release profiles (n=3 ± SD)

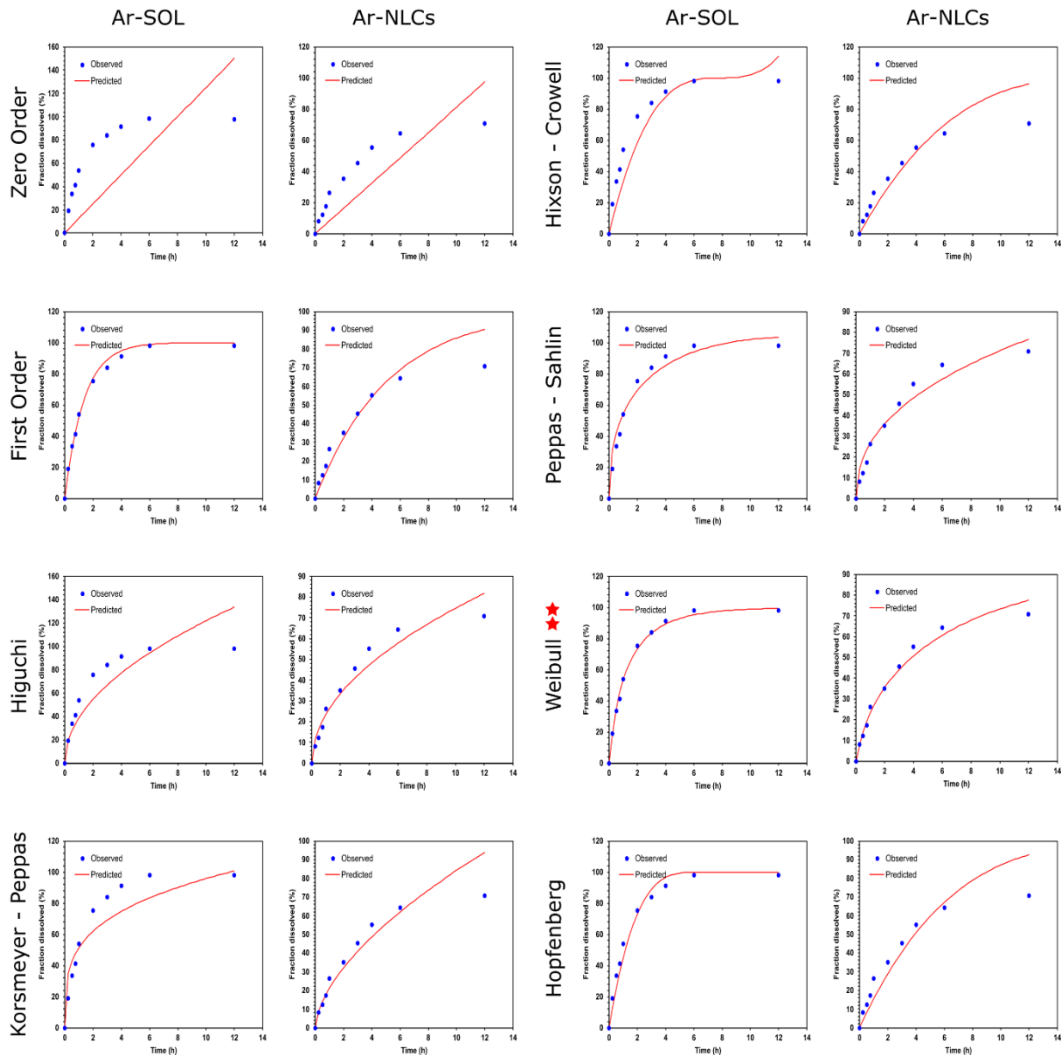

Figure 7. Release kinetics study for the Ar-SOL and Ar-NLCs.

Table 3. Release kinetics modelling of the Ar-SOL and Ar-NLCs.

Kinetic models and equations		Evaluation criteria				
		Parameter	r^2	r^2 adjusted	MSC	AIC
Zero-order kinetic model $F = k_0 * t$	Ar-SOL	k_0 = 12.499	-0.212	-0.212	-0.777	97.017
	Ar-NLCs	k_0 = 8.107	0.486	0.486	0.238	81.441
First-order kinetic model $F = 100 * [1 - \exp(-k_0 * t)]$	Ar-SOL	k_1 = 0.736	0.994	0.994	4.589	43.350
	Ar-NLCs	k_1 = 0.195	0.905	0.905	1.928	64.540
Higuchi kinetic model $F = k_H * t^{0.5}$	Ar-SOL	k_H = 38.517	0.768	0.768	0.876	80.484
	Ar-NLCs	k_H = 23.565	0.946	0.946	2.486	58.960
Korsmeyer-Peppas kinetic model $F = k_{KP} * t^n$	Ar-SOL	k_{KP} = 51.390	0.883	0.868	1.359	75.652
	Ar-NLCs	k_{KP} = 21.145	0.883	0.868	1.517	68.652
Hixson-Crowell kinetic model $F = 100 * [1 - (1 - kHC^t)^3]$	Ar-SOL	k_{HC} = 0.126	0.853	0.853	1.332	75.926
	Ar-NLCs	k_{HC} = 0.055	0.837	0.837	1.383	69.988
Peppas-Sahlin kinetic model $F = k_1 * t^m + k_2 * t^{2*m}$	Ar-SOL	k_1 = 64.417	0.960	0.949	2.243	66.816
	Ar-NLCs	k_1 = 27.140	0.952	0.938	2.203	61.784
Weibull kinetic model $F = 100 * \{1 - Exp[-((t - Ti)^{\beta})/\alpha]\}$	Ar-SOL	β = 0.730	0.996	0.995	4.634	42.903
	Ar-NLCs	**β = 0.670**	**0.982**	**0.977**	**3.211**	**51.708**
Hopfenberg kinetic model $F = 100 * [1 - (1 - k_{HB} * t)^n]$	Ar-SOL	k_{HB} = 0.148	0.975	0.971	2.889	60.357
	Ar-NLCs	k_{HB} = 0.037	0.865	0.848	1.373	70.092

2.5. Ex-vivo permeation studies

The porcine ear skin was employed to investigate the ex vivo permeability effectiveness of the Ar-NLCs and Ar-SOL. Results indicate that the Ar-NLCs exhibited higher permeability and flux over time compared to the Ar-SOL. The permeation of α-arbutin in Ar-NLCs were 13.041 ± 2.531 mg/cm², while only 5.071 ± 1.148 mg/cm² was permeated from the Ar-SOL. The Ar-NLCs had 2.53-fold greater permeability than the Ar-SOL (Figure 8 and Table 4).

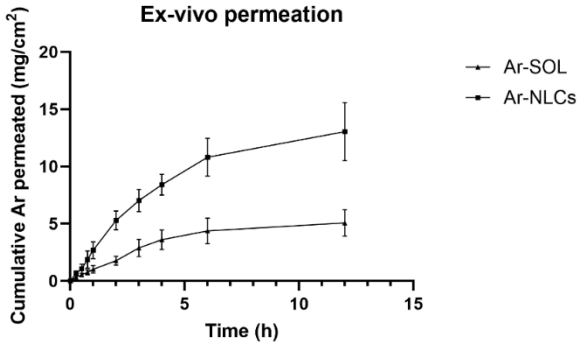

Figure 8. Ex-vivo permeation of Ar-SOL and the Ar-NLCs (n=3 ± SD).

Table 4. Flux and Permeability values of α-arbutin from the Ar-SOL and the Ar-NLCs (n=3 ± SD).

	Ar-SOL	Ar-NLCs
Permeability (P, cm/h)	0.045 ± 0.008	0.114 ± 0.017
Flux (J, mg/cm²/h)	0.449 ± 0.08	1.141 ± 0.174

2.6. Cytotoxicity assay

The cytotoxic effects of empty NLCs, α-arbutin (Ar), and Ar-NLCs were analyzed by MTT assay in the A375 cell line. Cell viability was evaluated using doses ranging from 31.5 - 500 µM for 24, 48, and 72 h to all groups (control, empty NLCs, pure α-arbutin (Ar), and Ar-NLCs), (Figure 9).

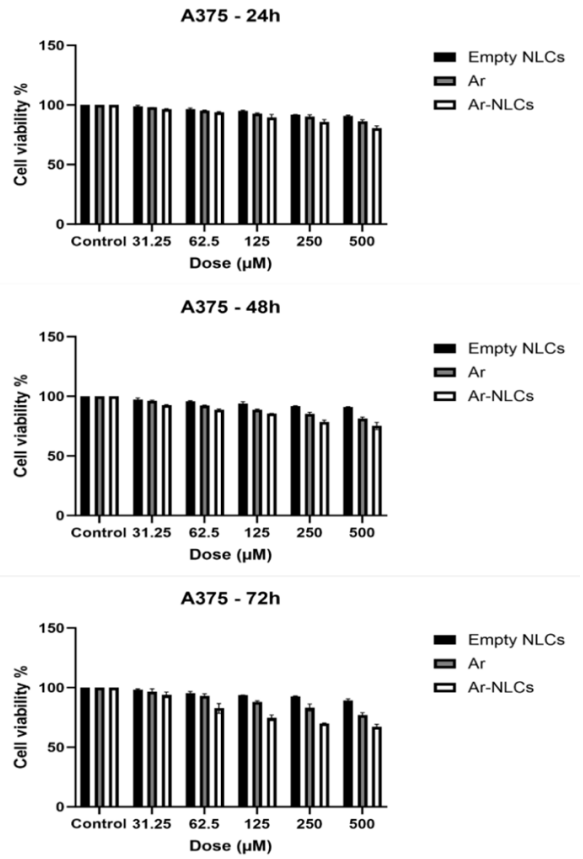

Figure 9. A375 cell viability for 24, 48, and 72 h.

2.7. Stability of Ar-NLCs

In this study, the Ar-NLCs were kept at 25°C for 3 months. The particle size and distribution revealed no significant changes (PDI < 0.3), suggesting preservation of uniform distribution (Table 5).

Table 5. Stability of Ar-NLCs at 25°C for 3 months (n=3 ± SD).

Months	Particle size (nm)	PDI	Zeta potential (mV)
0	228.7 ± 44.5	0.245 ± 0.03	-14.2 ± 2.64
1	236.1 ± 36.7	0.248 ± 0.03	-15.2 ± 3.83
3	244.4 ± 37.6	0.254 ± 0.02	-14.9 ± 3.11

3. DISCUSSION

Recent advancements in nanotechnology guided drug formulations to offer controlled release, target specific areas, and enhance transdermal drug delivery. The primary purpose of these treatments is to deliver the drug directly to the target site, reducing side effects and enhancing efficacy [13]. However, the transdermal delivery of hydrophilic drugs remains challenging. Consequently, different dosage formulations and application strategies are currently under investigation to address this issue.

In this research, the impact of independent factors on Ar-NLCs was evaluated using 3D surface-response graphs. Fabricated Ar-NLCs showed a particle size between 184.2 and 273.2 nm. The quadratic model was significant ($F=12.24$, $p<0.05$). Increasing the Gelucire 48/16:Castor oil ratio (X_1) resulted in larger particle sizes, while increasing Tween 80 (X_2) corresponded to a reduction in particle size (Eq. 1), as anticipated [14]. The PDI was between 0.217 to 0.273. The model was not statistically significant ($F=3.22$, $p>0.05$). The positive coefficient of X_1 (Eq. 2) suggests that an increasing amount of oil results in higher PDI and particle size of NLCs, as expected [15]. Additionally, the positive interaction term for X_2X_3 indicates that increasing amounts of Tween 80 and Capryol 90 result in higher PDI values, potentially leading to the formation of unwanted forms, like micelles. Similar results have been reported in other studies [16]. The zeta potential ranged from -16.84 to -11.56 mV and the model was significant ($F=18.02$, $p<0.05$). The zeta potential

decreased negatively with increasing amounts of Tween 80 [17]. In contrast, Capryol 90 had increased the zeta potential (Eq. 3). The combined use of surfactants and co-surfactants in NLCs plays a critical role, as it ensures an enhanced steric barricade, which is essential for the stability of NLCs [18].

Ensuring high entrapment of drugs in carriers is crucial, especially when incorporating a hydrophilic drug into a lipophilic carrier, which can be challenging. However, NLCs possess the unique capability to encapsulate both lipophilic and hydrophilic drug molecules [19]. The hydrophilic drug, α-arbutin, was successfully loaded into NLCs with an entrapment efficiency of 67.62 ± 4.46%.

The therapeutic effects of NLCs are mostly dependent on the controlled release of drugs. However, drugs can sometimes stick to the surface of NLCs and be rapidly released, a phenomenon known as burst release. This burst release is critical for preserving a therapeutic concentration in drug delivery systems for effective treatment [20]. In our study, α-arbutin showed burst effect in the first hour (26.249 ± 6.139%), followed by a sustained release (70.843 ± 9.242% after 12 hours). This behavior exemplifies a typical burst release. The α-arbutin release from NLCs was slower. The lipid matrix structure and surfactant concentrations within the NLC formulation can influence the release profile of α-arbutin [21].

The release behavior of the Ar-NLCs is best described by the Weibull model. This model had the highest values for r^2, adjusted r^2, and MSC, along with the lowest AIC values. In Weibull model, "β" value describes the release mechanism (Table 3). The Fickian diffusion was observed (β≤ 0.75). The "β" value was 0.670, confirming that the release of α-arbutin from the NLCs follows Fickian diffusion. Therefore, the Ar-NLCs can be regarded as showing sustained release [22]. Similar release behaviors were also observed in previous studies [21-24]. Bhaskar et al. [21] developed nitrendipine-loaded nanostructured lipid carriers (NLCs) and investigated their release kinetics as part of the characterization studies. They reported that drug release from the NLCs followed the Weibull kinetic model. Similarly, Mukta et al. [23] demonstrated that curcumin-loaded NLCs exhibited a biphasic drug release pattern in in vitro experiments, characterized by an initial burst release followed by sustained release. Their study also confirmed that the release kinetics of curcumin from the NLCs aligned with the Weibull model. In another study, Araujo et al. [24] developed curcumin-loaded NLCs and reported that the drug release from their formulation also adhered to Weibull kinetics.

The release behavior is a critical factor for drug delivery research, particularly during formulation development. The mathematical analysis of release profiles not only predicts in-vitro and in-vivo behavior, but also guides the selection of optimal carriers for targeted drug delivery. Lipid nanoparticles, with their complex release mechanisms involving diffusion, swelling, and erosion, are often described by the adaptable Weibull model. Moreover, factors such as particle size and morphology contribute to variations in release behavior, underscoring the need for detailed kinetic evaluations [25].

The Ar-NLCs showed higher flux and permeability compared to Ar-SOL (Table 4), which may be attributed to the lipophilicity of the Ar-NLCs, making skin penetration easier. Surfactants, known for enhancing permeability, also contribute to this effect [26]. The α-arbutin is hydrophilic and struggles to penetrate the skin effectively. Enhancing the lipophilicity of drug carriers improves the compatibility of drug molecules with the skin. The Ar-NLCs' enhanced permeability can be referable to their lipophilic character [27].

Nanoparticle based drug delivery systems present an innovative strategy for targeted drug delivery and sustained release. The primary purpose of targeting is to maintain the necessary drug concentration while minimizing toxicity and maximizing therapeutic effects. The NLCs have emerged as effective tools for enhancing bioavailability and permeability [19-21]. In our study, the higher cytotoxicity is attributed to the increased cellular uptake of α-arbutin. This increased cytotoxic effect (Figure 9) likely results from the ability of nanoparticles to deliver greater amounts of the α-arbutin directly to the cells [28]. Additionally, A375 cell viability demonstrated dose-dependent reduction, with the highest half maximal inhibitory concentration (IC_{50}) observed in the group treated with empty NLCs (236.4 μM). This means empty NLCs can be used safely. When comparing the IC_{50} values of Ar (152.6 μM) and Ar-NLCs (86.28 μM), an increase in cytotoxicity was determined, selectively affecting the A375 melanoma cell line. The decrease in cell viability followed a dose-dependent trend for both Ar (r^2 = 0.934) and Ar-NLCs (r^2 = 0.950), which is consistent with our study [29].

4. CONCLUSION

Quality by Design (QbD) has become a standard tool for comprehending and optimizing pharmaceutical products and their production processes. It enables the screening and optimization of

formulations by investigating how independent variables impact the product's performance. In this study, the QbD methodology was applied to the fabrication of α-arbutin loaded NLCs, a hydrophilic drug delivery system. Ar-NLCs were produced using a high shear homogenization-ultrasonication method. The critical process parameters and their effects on quality attributes were systematically analyzed using a Box-Behnken design to optimize the formulation. Optimized Ar-NLCs exhibited a particle size of 228.7 ± 44.5 nm and an entrapment efficiency of 67.62 ± 4.46% respectively. Release kinetic studies revealed that the Ar-NLCs followed the Weibull kinetic model, releasing α-arbutin through Fickian diffusion with sustained release characteristics. Additionally, the Ar-NLCs achieved 2.53-fold greater drug diffusion compared to α-arbutin solution (Ar-SOL). The Ar-NLCs were determined to have higher cytotoxic effects than Ar-SOL. These findings underscore the effectiveness of the NLC-based colloidal carrier systems with enhanced formulation quality and improved transdermal drug delivery.

5. MATERIALS AND METHODS

Methanol, acetonitrile, tween 80 and α-arbutin were obtained from Merck (Germany), Gelucire 48/16, Precirol ATO 5, Compritol 888 ATO, Labrasol, Plurol Oleique CC 497, Capryol 90, Capryol PGMC, Lauroglycol 90 were generously provided by Gatte-Fosse (France). Jojoba oil, Castor oil and St John's Wort oil were purchased from Talya (Türkiye). A375 cell line (A375 - malign melanoma cells) was obtained from ATCC (USA). The other chemicals used in studies were analytical grade.

5.1. Methods

5.1.1. Determination of α-arbutin

A high-performance liquid chromatography (HPLC, Shimadzu, Japan) with a reverse phase C18 column (5 µm, 250 mm × 4.6 mm) was utilized to determine the α-arbutin. The mobile phase consisted of a water:methanol mixture (90:10, v/v), with a flow rate of 0.6 mL/min. The injection volume was 20 µL. The analysis was conducted at 286 nm wavelength [30]. The α-arbutin solutions were prepared in methanol at concentrations ranging from 20 to 200 µg/mL. The study was conducted at 25°C.

5.1.2. Selection of lipids and surfactants

A primary focus in the development of NLCs is determining the drug solubility in lipids. This step is crucial as it directly affects drug loading, encapsulation, and the overall effectiveness of lipid carriers in delivering therapeutic agents. As expected, when a drug exhibits high solubility in the lipid phase, higher loading capacity and encapsulation efficiency can be achieved [31].

The solid lipids are chosen based on their association for the drug and their physical compatibility with liquid lipids. To assess this, an extra amount of α-arbutin was added to 2 mL of water in test tubes until saturation was reached. After filtering out the undissolved drug, 1 g of solid lipid (Gelucire 48/16, Compritol 888 ATO, and Precirol ATO 5) was submitted into test tubes. Then, the tubes were placed in a shaking water bath (Witeg, Germany) at 80°C for 12 hours before being cooled to 25°C. Once the solid lipids had frozen, they were removed, and the percentage of drug trapped in the solid lipids was calculated from the amount of drug dissolved in water. Additionally, a piece of solid lipid-drug mixture was examined under light microscopy to check for the presence of drug crystals [32-34].

The evaluation of liquid lipids and surfactants for the formulation is based on the solubility of the drugs. To assess this, a fixed volume (1 mL) of various oils (Jojoba oil, St. John's Wort oil, and Castor oil) and surfactants (Capryol 90, Capryol PGMC, Plurol Oleique CC 497, Lauroglycol 90, Labrasol, and Tween 80) was placed in separate 10 mL glass vials. Extra amount of α-arbutin was added, and the vials were incubated in a shaking water bath (Witeg, Germany) at 37°C and 100 rpm for 72 hours. Afterward, the vials were centrifuged for 30 minutes at 6000 rpm (Hettich, Germany) to remove undissolved drug. The supernatant was collected, and the solubility of α-arbutin in surfactants and liquid lipids was determined [32-34] using the HPLC method described previously.

The binary mixture of solid/liquid lipids was determined based on the preliminary solubility study performed as described above. The solid (Gelucire 48/16) and liquid lipids (Castor oil) with the highest dissolving capacity of α-arbutin were taken and mixed in different ratios from 9:1 to 1:9 to determine the miscibility of lipids. The mixture was stirred for 1 h at 55°C with a magnetic stirrer at 100 rpm and then

cooled and kept at 25°C for a day. Afterward, the lipid mixture was examined under a light microscope to determine whether phase separation had occurred [32-34].

5.1.3. Preparation of α-arbutin loaded nanostructured lipid carriers (Ar-NLC)

To assess the impact of components on NLCs, Box-Behnken design (BBD) was employed. The independent factors (solid and liquid oils and surfactants) and dependent variables (particle size and distribution, and zeta potential) were analyzed. The Design-Expert (software version 12.0.3, Stat-Ease Inc., USA) was employed. Gelucire 48/16: Castor oil (8:2), (X_1, 10-30%), Tween 80 (X_2, 1-5%) and Capryol 90 (X_3, 1-5%) ratios were determined as independent factors. Dependent factors were determined to have minimum for particle size, polydispersity index (Y_1, Y_2), and maximum for zeta potential (Y_3). Levels were numbered (Table 1) and results were evaluated with the quadratic model (Eq. 1).

Table 6. Factors employed in experimental design

Independent factors	**Levels**		
	Low (-1)	**Medium (0)**	**High (+1)**
X_1 = Amount of lipid (Gelucire 48/16:Castor oil, 8:2) (%)	10	20	30
X_2 = Amount of Tween 80 (%)	1	3	5
X_3 = Amount of Capryol 90 (%)	1	3	5
Dependent factors		**Desired**	
Y_1 = Particle size (nm)		Minimum	
Y_2 = Polydispersity index (PDI)		Minimum	
Y_3 = Zeta potential (mV)		Maximum	

$$\mathbf{Y=}\ \delta_0+\delta_1X_1+\delta_2X_2+\delta_3X_3+\delta_4X_1^2+\delta_5X_1X_2+\delta_6X_1X_3+\delta X_2^2+\delta_8X_2X_3+\delta_9X_3^2 \qquad \text{(Eq. 1)}$$

According to this, Y was the response, X_1-X_3 were the independent variables, δ_0 was the intercept, and δ_1-δ_9 were the regression coefficients (ANOVA).

The mixture of lipids (Gelucire 48/16:Castor oil, 8:2) was heated slightly above the melting point (55°C). Capryol 90 and α-arbutin were added separately to this melted lipid mixture to form the oil phase. The water phase containing Tween 80 and distilled water was also brought to the 55°C. When both phases reached to the same temperature, the oil phase was poured into the water phase to form an emulsion. This emulsion was homogenized at 10000 rpm for five minutes (Velp OV5, Italy), then was ultrasonicated at 40 W power, 20 kHz for five minutes (Bandalin Sonopuls HD 4100, Germany). After the ultrasonication step, the dispersion was cooled in an ice bath until it reached 25°C, and then stored at 4°C [35].

5.1.4. Characterization studies of Ar-NLC

The Ar-NLCs were diluted (1:20) with distilled water, and the particle size (ps), polydispersity index (PDI), and zeta potential (zp) were determined (Malvern Nano ZS, UK). Scanning electron microscopy (SEM) images of the Ar-NLCs were investigated (DUBTAM, Dicle University). Scanning was conducted under low vacuum conditions at 10 kV and 40000-100000 magnification. The samples were diluted in distilled water (1:1000), seated on a grid, and allowed to dry for 24 h at 25°C before the study. To Ar-NLCs were centrifuged at 16000 rpm at 0°C for 30 min. The supernatant was filtered (0.22 µm PVDF). The free α-arbutin portion was calculated (n=3, mean ± SD), then the entrapment efficiency (EE%) was determined (Eq. 4).

$$\text{Entrapment efficiency\%} = {}^{Ar_0\text{-}Ar_1}/_{Ar_0} \times 100 \qquad \text{(Eq. 4)}$$

Ar_0 was the total amount of α-arbutin, and Ar_1 was the amount of free α-arbutin.

5.1.5. Differential scanning calorimetry (DSC) and Fourier transform infrared (FTIR) studies

DSC and FTIR analyses were conducted to determine the possible incompatibility between the formulation components. Gelucire 48/16, α-arbutin, and a physical blend (α-arbutin and Gelucire 48/16:Castor oil (8:2)) were examined using differential scanning calorimetry (DSC 60, Shimadzu, Japan).

The samples were compressed, locked in aluminum pans, and heated at a rate of 10°C/min from 25°C to 300°C to evaluate their thermal behavior [36]. To conduct Fourier transform infrared spectroscopy (FTIR) analysis (Agilent Cary 630, Agilent, USA), the samples were scanned across the infrared spectrum from 400 to 4000 cm^{-1} with a resolution of 4 cm^{-1}.

5.1.6. Investigation of release and kinetics

In this study, the Franz diffusion cells (cell diameter 1 cm^2) were employed. Before the experiment, a dialysis bag (Mwco=12000) soaked in phosphate buffered saline (PBS, pH 7.4) for 6 hours. Ar-SOL and Ar-NLCs (containing 20 mg of α-arbutin) were filled into the donor chamber. The PBS (10 mL) was loaded to the receptor chamber. Studies were conducted at 37°C with mixing at 100 rpm continuously. At the indicated times (0, 0.25, 0.5, 0.75, 1, 2, 4, 6, and 12 h) 0.5 mL of samples were collected, and an equivalent amount of fresh PBS was added to preserve the sink condition. The amount of α-arbutin in samples was determined (n=3, mean ± SD).

The release profile of α-arbutin from Ar-SOL and Ar-NLCs were evaluated with the DDSolver software program. Mathematical kinetic models were applied to determine the release kinetics of α-arbutin from NLCs. The Akaike information criterion (AIC), along with the coefficient (r^2), adjusted coefficient (r^2 adjusted), and model selection criteria (MSC) were determined to select the most appropriate model for the data [37].

5.1.7. Ex-vivo permeation studies

The Franz diffusion cells with the porcine ear skin were used for permeability studies (diffusion area of 1 cm^2). Ar-SOL and Ar-NLCs (each containing 20 mg of α-arbutin) were applied on to the porcine ear skin. The acceptor compartment was filled with 10 mL of PBS (pH 7.4). Studies were performed at 37°C with mixing at 100 rpm continuously. At the indicated times (0, 0.25, 0.5, 0.75, 1, 2, 4, 6, and 12 h) 0.5 mL of samples were collected, and an equivalent amount of fresh PBS was added. The sink condition was preserved. The permeability (P), and flux (J) values of α-arbutin was calculated (Eq. 5).

$$M/S = D.K.Cd/h.t \qquad \text{(Eq. 5)}$$

S was the membrane surface area (cm^2), and M was the diffused amount of α-arbutin (mg). D was the diffusion coefficient of α-arbutin (cm^2/h). K was the partition coefficient of α-arbutin, Cd was the of α-arbutin concentration in the donor cell, h was the membrane thickness, and t was the time (hour), (n=3, mean ± SD).

5.1.8. Cytotoxicity assay

The cytotoxicity assay was conducted using A375 cell line (A375-CRL-1619, human, malignant melanoma cells, American Type Cell Culture, USA). A375 cells were inoculated in a 96-well plate in 200 µL of Dulbecco's modified Eagle's Medium (DMEM), supplemented with 2mM glutamine and 15% Fetal Bovine serum (FBS) and incubated in 5% CO_2 environment at 37°C for 48 hours. After the incubation period, cells were exposed to different concentrations (31.25, 62.5, 125, 250 and 500 µg/mL) of Ar, Empty NLCs and Ar-NLCs in PBS (20 µL). Then, cells were incubated for 24, 48 and 72 h in in 5% CO_2 atmosphere at 37°C. After the treatment, formulations were removed from wells. Then, 20 µL of 3-(4,5-dimethylthiazol-1-yl)-2,5-diphenyltetrazolium bromide (MTT) solution (5 mg/mL in PBS) were added to wells, followed by 3 h incubation in 5% CO_2 environment at 37°C. The MTT solution was disarded, and 100 µL dimethyl sulfoxide (DMSO) was added to solubilize crystals. The absorbance was determined (Rayto RT-2100C, China) at 570 nm. The cell viability% (Eq. 6) was determined [38].

$$\text{Cell viability\%} = \left[\frac{\text{Sample absorbance value}}{\text{Control absorbance value}}\right] \times 100 \qquad \text{(Eq. 6)}$$

5.1.9. Stability of Ar-NLCs

Following three months of storage at 25°C, Ar-NLCs were investigated for particle size, zeta potential and polydispersity index (n=3, mean ± SD).

5.1.10. Statistical analysis

Experiments were performed three times (n=3) to provide accuracy. Results were reported as mean ± standard deviation (mean ± SD). A one-way ANOVA test was performed to determine the statistical significance ($p<0.05$).

Acknowledgements: Authors would like to thank Dicle University Science and Technology Application and Research Center (DUBTAM).
Author contributions: Concept – MO.T.; Design – MO.T., İ.S.; Supervision – MO.T.; Resources – MO.T., İ.S.; Materials – MO.T., İ.S.; Data Collection and/or Processing – MO.T., İ.S.; Analysis and/or Interpretation – MO.T., İ.S.; Literature Search – MO.T., İ.S.; Writing – MO.T., İ.S.; Critical Reviews – MO.T., İ.S.
Conflict of interest statement: The authors declare that they have no competing interests.

REFERENCES

[1] Boo YC. Arbutin as a skin depigmenting agent with antimelanogenic and antioxidant properties. Antioxidants. 2021; 10(7): 1129-1140. https://doi.org/10.3390/antiox10071129
[2] Apalla Z, Nashan D, Weller RB, Castellsagué X. Skin cancer: epidemiology, disease burden, pathophysiology, diagnosis, and therapeutic approaches. Dermatol Ther. 2017; 7: 5-19. https://doi.org/10.1007/s13555-016-0165-y
[3] Huang J, Chan SC, Ko S, Lok V, Zhang L, Lin X, Wong MC. Global incidence, mortality, risk factors and trends of melanoma: a systematic analysis of registries. Am J Clin Dermatol. 2023; 24(6): 965-975. https://doi.org/10.1007/s40257-023-00795-3
[4] Liu JK. Natural products in cosmetics. Nat Prod Bioprospect. 2022; 12(1): 40-82. https://doi.org/10.1007/s13659-022-00363-y
[5] Li Z, Wang Z, Zhou Q, Wang R, Xiong Z, Wu Y, Shu P. The molecular mechanisms underlying optical isomer arbutin permeating the skin: The molecular interaction between arbutin and skin components. International Journal of Pharmaceutics. 2024; 664, 124584. https://doi.org/10.1016/j.ijpharm.2024.124584
[6] Tofani RP, Sumirtapura YC, Darijanto ST. Formulation, characterisation, and in vitro skin diffusion of nanostructured lipid carriers for deoxyarbutin compared to a nanoemulsion and conventional cream. Sci Pharm. 2016; 84(4): 634-645. https://doi.org/10.3390/scipharm84040634
[7] Raza K, Singh B, Lohan S, Sharma G, Negi P, Yachha Y, Katare OP. Nano-lipoidal carriers of tretinoin with enhanced percutaneous absorption, photostability, biocompatibility and anti-psoriatic activity. Int J Pharm. 2013; 456(1): 65-72. https://doi.org/10.1016/j.ijpharm.2013.08.019
[8] Bastogne T. Quality-by-design of nanopharmaceuticals–a state of the art. Nanomedicine: Nanotechnol Biol Med. 2017; 13(7): 2151-2157. https://doi.org/10.1016/j.nano.2017.05.014
[9] Saeedi M, Rezanejad Gatabi Z, Morteza-Semnani K, Rahimnia SM, Yazdian-Robati R, Hashemi SMH. Preparation of arbutin hydrogel formulation as green skin lightener formulation: in vitro and in vivo evaluation. J Dispers Sci Technol. 2024; 1-13. https://doi.org/10.1080/01932691.2024.2371954
[10] Shinde UK, Suryawanshi DG, Amin PD. Development of Gelucire® 48/16 and TPGS mixed micelles and its pellet formulation by extrusion spheronization technique for dissolution rate enhancement of curcumin. AAPS PharmSciTech. 2021; 22(5): 182-192. https://doi.org/10.1208/s12249-021-02032-8
[11] Alshawwa SZ, El-Masry TA, Elekhnawy E, Alotaibi HF, Sallam AS, and Abdelkader DH. Fabrication of Celecoxib PVP microparticles stabilized by Gelucire 48/16 via electrospraying for enhanced anti-inflammatory action. Pharmaceuticals 2023; 16(2): 258-275. https://doi.org/10.3390/ph16020258
[12] Ahmad U, Naqvi SR, Ali I, Saleem F, Mehran MT, Sikandar U, Juchelková D. Biolubricant production from castor oil using iron oxide nanoparticles as an additive: Experimental, modelling and tribological assessment. Fuel. 2022; 324, 124565. https://doi.org/10.1016/j.fuel.2022.124565
[13] Zhou X, Hao Y, Yuan L, Pradhan S, Shrestha K, Pradhan O, Liu H, Li W. Nano-formulations for transdermal drug delivery: A review. Chin Chem Lett. 2018; 29: 1713–1724. https://doi.org/10.1016/j.cclet.2018.10.037
[14] Han F, Li S, Yin R, Liu H, Xu L. Effect of surfactants on the formation and characterization of a new type of colloidal drug delivery system: Nanostructured lipid carriers. Colloid Surf A: Physicochem Eng Aspect. 2008; 315(1-3): 210-216. https://doi.org/10.1016/j.colsurfa.2007.08.005
[15] Bashiri S, Ghanbarzadeh B, Ayaseh A, Dehghannya J, Ehsani A, Ozyurt H. Essential oil-loaded nanostructured lipid carriers: The effects of liquid lipid type on the physicochemical properties in beverage models. Food Biosci. 2020; 35: 100526. https://doi.org/10.1016/j.fbio.2020.100526
[16] Tan SW, Billa N, Roberts CR, Burley JC. Surfactant effects on the physical characteristics of Amphotericin B-containing nanostructured lipid carriers. Colloid Surf A: Physicochem Eng Aspect. 2010; 372(1-3): 73-79. https://doi.org/10.1016/j.colsurfa.2010.09.030
[17] Witayaudom P, Klinkesorn U. Effect of surfactant concentration and solidification temperature on the characteristics and stability of nanostructured lipid carrier (NLC) prepared from rambutan (*Nephelium lappaceum* L.) kernel fat. J Colloid Interface Sci. 2017; 505: 1082-1092. https://doi.org/10.1016/j.jcis.2017.07.008

[18] Pogorzelski S, Watrobska-Swietlikowska D, Sznitowska M. Surface tensometry studies on formulations of surfactants with preservatives as a tool for antimicrobial drug protection characterization. J Biophys Chem. 2012; 3(04): 324-333. https://doi.org/10.4236/jbpc.2012.34040

[19] Souto EB, Baldim I, Oliveira WP, Rao R, Yadav N, Gama FM, Mahant S. SLN and NLC for topical, dermal, and transdermal drug delivery. Expert Opin Drug Deliv. 2020; 17(3): 357-377. https://doi.org/10.1080/17425247.2020.1727883

[20] Nagaich U, Gulati N. Nanostructured lipid carriers (NLC) based controlled release topical gel of clobetasol propionate: Design and in vivo characterization. Drug Deliv Transl Res. 2016; 6: 289-298. https://doi.org/10.1007/s13346-016-0291-1

[21] Bhaskar K, Krishna Mohan C, Lingam M, Prabhakar Reddy V, Venkateswarlu V, Madhusudan Rao Y. Development of nitrendipine controlled release formulations based on SLN and NLC for topical delivery: in vitro and ex vivo characterization. Drug Develop Ind Pharm. 2008; 34(7): 719-725. https://doi.org/10.1080/03639040701842485

[22] Toksoy MO, Aşır F, Güzel MC. Quality by design approach for development and characterization of gabapentin-loaded solid lipid nanoparticles for intranasal delivery: In vitro, ex vivo, and histopathological evaluation. Iran J Basic Med Sci. 2024; 27(7): 904-913. 10.22038/IJBMS.2024.76281.16511

[23] Agrawal M, Saraf S, Pradhan M, Patel RJ, Singhvi G, Alexander A. Design and optimization of curcumin loaded nano lipid carrier system using Box-Behnken design. Biomed Pharmacother. 2008; 141: 111919. https://doi.org/10.1016/j.biopha.2021.111919

[24] Araujo VHS, da Silva PB, Szlachetka IO, da Silva SW, Fonseca-Santos B, Chorilli M, Muehlmann LA. The influence of NLC composition on curcumin loading under a physicochemical perspective and in vitro evaluation. Colloid Surf A: Physicochem Eng Aspect. 2020; 602: 125070. https://doi.org/10.1016/j.colsurfa.2020.125070

[25] Porbaha P, Ansari R, Kiafar MR, Bashiry R, Khazaei MM, Dadbakhsh A, Azadi AA. comparative mathematical analysis of drug release from lipid-based nanoparticles. AAPS PharmSciTech. 2024; 25(7): 208. https://doi.org/10.1208/s12249-024-02922-7

[26] Dai W, Zhang D, Duan C, Jia L, Wang Y, Feng F, Zhang Q. Preparation and characteristics of oridonin-loaded nanostructured lipid carriers as a controlled-release delivery system. J Microencapsul. 2010; 27(3): 234-241. https://doi.org/10.3109/02652040903079526

[27] Nguyen CN, Nguyen TTT, Nguyen HT, Tran TH. Nanostructured lipid carriers to enhance transdermal delivery and efficacy of diclofenac. Drug Deliv Transl Res. 2017; 7: 664-673. https://doi.org/10.1007/s13346-017-0415-2

[28] Elgizawy HA, Ali AA, Hussein MA. Resveratrol: Isolation, and its nanostructured lipid carriers, inhibits cell proliferation, induces cell apoptosis in certain human cell lines carcinoma and exerts protective effect against paraquat-induced hepatotoxicity. J Med Food. 2021; 24(1): 89-100. https://doi.org/10.1089/jmf.2019.028

[29] Cheng SL, Liu RH, Sheu JN, Chen ST, Sinchaikul S, Tsay GJ. Toxicogenomics of A375 human malignant melanoma cells treated with arbutin. J Biomed Sci. 2007; 14: 87-105. https://doi.org/10.1007/s11373-006-9130-6

[30] Aung NN, Ngawhirunpat T, Rojanarata T, Patrojanasophon P, Opanasopit P, Pamornpathomkul B. HPMC/PVP dissolving microneedles: A promising delivery platform to promote trans-epidermal delivery of alpha-arbutin for skin lightening. AAPS PharmSciTech. 2020; 21: 25-37. https://doi.org/10.1208/s12249-019-1599-1

[31] Subramaniam B, Siddik ZH, Nagoor NH. Optimization of nanostructured lipid carriers: Understanding the types, designs, and parameters in the process of formulations. J Nanoparticle Res. 2020; 22: 1-29. https://doi.org/10.1007/s11051-020-04848-0

[32] Bajwa N, Mahal S, Naryal S, Singh PA, Baldi A. Development of novel solid nanostructured lipid carriers for bioavailability enhancement using a quality by design approach. AAPS PharmSciTech. 2022; 23(7): 253-266. https://doi.org/10.1208/s12249-022-02386-7

[33] Kim BS, Na YG, Choi JH, Kim I, Lee E, Kim SY, Cho CW. The improvement of skin whitening of phenylethyl resorcinol by nanostructured lipid carriers. Nanomaterials. 2017; 7(9): 241-257. https://doi.org/10.3390/nano7090241

[34] Negi LM, Jaggi M, Talegaonkar S. Development of protocol for screening the formulation components and the assessment of common quality problems of nano-structured lipid carriers. Int J Pharm. 2014; 461(1-2): 403-410. https://doi.org/10.1016/j.ijpharm.2013.12.006

[35] Subroto E, Andoyo R, Indiarto R. Solid lipid nanoparticles: Review of the current research on encapsulation and delivery systems for active and antioxidant compounds. Antioxidants. 2023; 12(3): 633-660. https://doi.org/10.3390/antiox12030633

[36] Saeedi M, Rezanejad Gatabi Z, Morteza-Semnani K, Rahimnia SM, Yazdian-Robati R, Hashemi SMH. Preparation of arbutin hydrogel formulation as green skin lightener formulation: in vitro and in vivo evaluation. J Dispers Sci Technol. 2024; 1-13. https://doi.org/10.1080/01932691.2024.2371954

[37] Gamal A, Saeed H, El-Ela FIA, Salem HF. Improving the antitumor activity and bioavailability of sonidegib for the treatment of skin cancer. Pharmaceutics. 2021; 13(10): 1560-1575. https://doi.org/10.3390/pharmaceutics13101560

[38] Ergin AD, Oltulu Ç, Koç B. Enhanced cytotoxic activity of 6-mercaptopurine–loaded solid lipid nanoparticles in hepatic cancer treatment. ASSAY Drug Develop Technol. 2023; 21(5): 212-221. https://doi.org/10.1089/adt.2023.00